

## A NOVEL ACTUATION MECHANISM BASED ON FERROMAGNETIC SMA THIN FILMS

M. Kohl, D. Brugger, M. Ohtsuka\* and T. Takagi\*

Forschungszentrum Karlsruhe GmbH, Postfach 3640, 76021 Karlsruhe, Germany  
Tel.: +49 7247 822798, FAX: +49 7247 824331, e-mail: manfred.kohl@imt.fzk.de

\* Tohoku University, 2-1-1 Katahira, Aoba-ku, Sendai 980-8577, Japan

### ABSTRACT

A novel actuation mechanism is presented, which makes use of the antagonism of intrinsic magnetic and shape recovery forces acting on a ferromagnetic shape memory alloy (SMA) microactuator in a magnetic field. This mechanism is associated with large actuation and small biasing forces in each actuation direction resulting in a large stroke. Since no external biasing elements are required, extremely compact designs are possible. As a demonstrator, an optical microscanner of  $9 \times 3 \times 5 \text{ mm}^3$  size is presented showing large scanning angles up to 75 deg in off-resonance mode. The scanning performance keeps frequency-independent below a critical frequency, which is determined by heat-transfer times.

### INTRODUCTION

Recently, ferromagnetic SMAs have gained considerable attention, as they exhibit an interesting combination of thermoelastic and magnetic properties. One novel transducer mechanism observed in these material systems is the magnetic field-induced rearrangement of martensitic variants, commonly referred to as magnetic shape memory (MSM) effect [1-5]. Recent studies on this effect in bulk single crystals of  $\text{Ni}_2\text{MnGa}$  revealed considerable shape changes up to 6 % and interesting response times of several ms [5]. Other transducer mechanisms have been proposed for the development of actuators, which depend e.g. on a magnetic field-induced martensitic phase transformation [6], on a temperature-dependent change of magnetic moment [7] or on a temperature-dependent change of magnetoelastic interaction [7].

For microsystems applications, thin films or sheets of ferromagnetic shape memory alloys are of particular interest. Recently,  $\text{Ni}_2\text{MnGa}$  thin films have been successfully fabricated by magnetron sputtering [8-10]. This paper describes how the intrinsic magnetic and shape recovery forces available in these materials can be implemented in an actuation mechanism to generate large work outputs in small dimensions. After discussion of material properties and actuation mechanism, an optical microscanner is presented as a demonstrator.

### MATERIAL PROPERTIES

Ferromagnetic thin films of  $\text{Ni}_2\text{MnGa}$  have been deposited on an alumina substrate by RF magnetron sputtering. The sputtering target of nominal composition  $\text{Ni}_{52}\text{Mn}_{24}\text{Ga}_{24}$  has been fabricated by hot pressing. During sputtering the

substrate temperature has been kept at 323 K. An Argon gas flow has been maintained at  $230 \text{ mm}^3\text{s}^{-1}$ . The RF power has been adjusted between 50 and 400 W, which affects the Ni content and thus the phase transformation temperatures of the thin films [8]. As-deposited thin films have been annealed at 1073 K for 36 ks to crystallize the films and to adjust the planar memory shape. Detailed investigations of the chemical compositions, crystal structures and magnetic properties have been presented in previous publications [8,9].

Fig. 1 shows the dependence of Curie temperature  $T_C$  and martensitic start transformation temperature  $M_s$  on the Ni content in thin film and bulk specimens. The  $M_s$  temperature increases by more than 120 K for increasing Ni content from 50 to 54 mol%, which is attributed to an increase of conduction electron density stabilizing the low-temperature tetragonal phase [6]. In contrast, the Curie temperature is much less affected. The thin films show the same dependency as the bulk specimens even though a larger scattering of data is present. In both cases,  $T_C$  and  $M_s$  temperature merge for a Ni content above 54 mol%. As a consequence, a mixed phase transition occurs from paramagnetic austenite to ferromagnetic martensite [6].

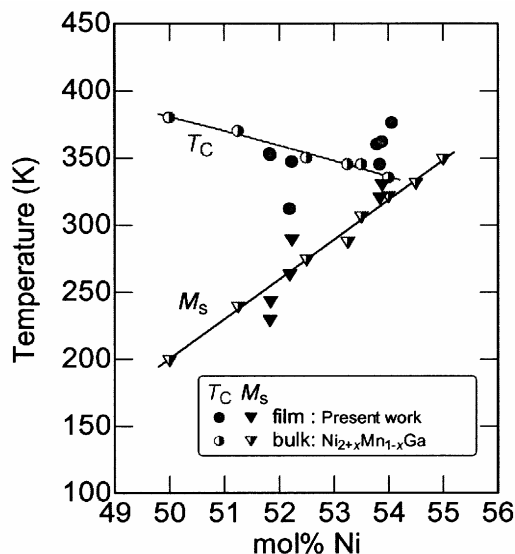


Fig. 1: Curie temperature  $T_C$  and martensitic start transformation temperature  $M_s$  as a function of Ni content of  $\text{Ni}_2\text{MnGa}$  bulk and thin film specimens.

For fabrication of optical scanners thin films with the stoichiometry  $\text{Ni}_{54.0}\text{Mn}_{24.1}\text{Ga}_{21.9}$  have been used displaying

the one-way shape memory effect. The corresponding phase transformation and Curie temperatures are summarized in Table 1. The phase transformation temperatures have been determined by differential scanning calorimetry, electrical resistance and mechanical bending measurements. The Curie temperatures have been determined from magnetic permeability measurements [9]. The film thickness is 10  $\mu\text{m}$ .

Table 1: Phase transformation and Curie temperatures (Kelvin) of thin films used for fabrication of optical scanners. The start and finish temperatures of the martensitic and corresponding reverse transformation are denoted as  $M_s$ ,  $M_f$ ,  $A_s$  and  $A_f$ , respectively. The stoichiometry indicates the film composition.

Specimen	$M_s$	$M_f$	$A_s$	$A_f$	$T_C$
Ni <sub>54.0</sub> Mn <sub>24.1</sub> Ga <sub>21.9</sub> Sputtering power: 50 W	373	365	387	397	376

### ACTUATION MECHANISM

The basic idea of the proposed actuation mechanism is to use both magnetic and shape recovery forces either for actuation or biasing depending on the actuation direction. In ferromagnetic shape memory alloys, both forces are available as an intrinsic material property. Since the material exhibits a ferromagnetic and a martensitic phase transformation, these forces can be controlled by heating / cooling the material above / below the corresponding phase transformation temperatures. In particular, for Ni<sub>2</sub>MnGa thin film specimens with Ni content above about 54 mol%, a direct phase transformation from paramagnetic austenite to ferromagnetic martensite is obtained. This feature can be favorably exploited to realize a perfect antagonism, where the magnetic force is large in the case of small shape recovery force and vice versa.

The proposed actuation mechanism may be applied to generate bending, torsion or tensile motion, including any combination of them. Fig. 1 illustrates the actuation mechanism for the case of a bending microactuator consisting of a double-beam structure. The microactuator is mounted in a magnetic circuit consisting of a permanent magnet and a soft-magnetic core. Electrical interconnections are provided for direct electrical heating.

When no heating current is applied, the microactuator is in a ferromagnetic and martensitic condition. In this case, the magnetic reluctance force  $F_{mag}$  dominates, while the biasing force  $F_{mart}$  is very low due to the high compliance in martensitic condition. As a result, the double-beam end is deflected to close the magnetic circuit (Fig. 2a).

By heating the microactuator above the temperatures of ferromagnetic and martensitic reverse transformation, the microactuator becomes paramagnetic and austenitic. Thus, the magnetic force strongly decreases, while at the same time a strong shape recovery force  $F_{SME}$  occurs in opposite direction. In this case, a reverse biasing behavior is present characterized by a decrease of biasing force as a

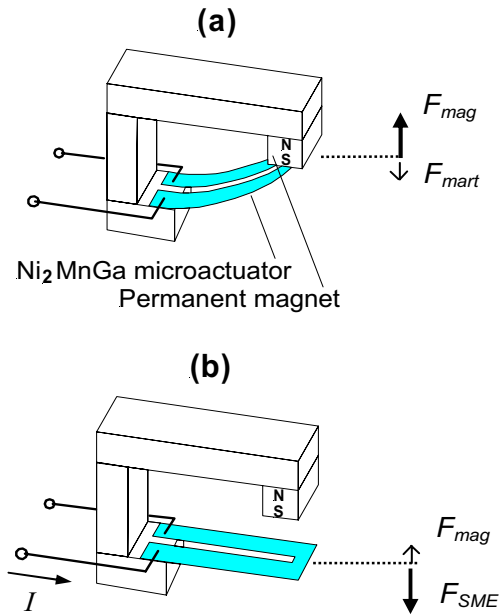


Fig. 2: Schematic of the proposed actuation mechanism. N and S denote north and south pole of the permanent magnet,  $I$  denotes electrical current.

function of displacement in actuation direction. As a consequence, the double-beam moves to its planar memory shape (Fig. 2b).

Since the bi-directional actuation is associated with a high net-force in both directions, a large stroke is obtained. Due to the use of an intrinsic antagonism, no reset spring or other external biasing elements are required allowing extremely compact and simple designs, which can be miniaturized to a great extent.

For the presented actuator design, application of an alternating current results in a periodic oscillation of the double beam. By attaching a small mirror at the front end of the beam, this motion may be used for scanning of a collimated light beam. Thus, an optical microscanner has been developed as a demonstrator for the proposed actuation mechanism.

### OPTICAL MICROSCANNER

#### Fabrication

Bending microactuators have been fabricated by photochemical micromachining of the thin films. Between thin film and substrate a sacrificial layer has been introduced in order to release the microactuators after micromachining. The dimensions of the double beams without bond pads are  $5 \times 0.5 \times 0.01 \text{ mm}^3$ . Micromirrors of  $1.5 \times 1.5 \times 0.25 \text{ mm}^3$  size have been fabricated by coating of a silicon wafer with Au in a sputtering apparatus and subsequent dicing. The magnet and magnetic core have been machined by spark erosion. Finally, the components have been assembled by adhesive bonding. Electrical contacts have been made by laser welding. Fig. 3 shows a

prototype of the optical microscanner. The overall size is about  $9 \times 3 \times 5 \text{ mm}^3$ .

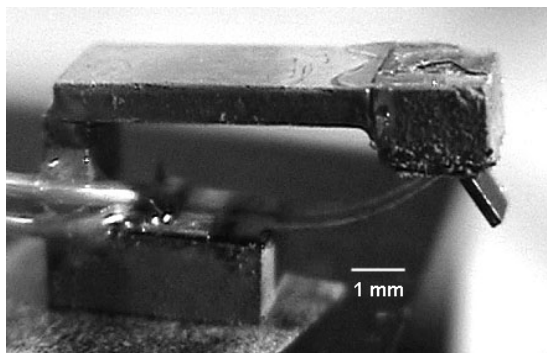


Fig. 3: Prototype of an optical microscanner based on the proposed actuation mechanism. The thickness of the  $\text{Ni}_2\text{MnGa}$  microactuator is  $10 \mu\text{m}$ .

#### Mechanical performance of the $\text{Ni}_2\text{MnGa}$ microactuator

Stationary beam bending characteristics of the  $\text{Ni}_2\text{MnGa}$  microactuator have been determined by beam bending experiments in a thermostat. The ambient temperature has been ramped step-wise with sufficient waiting time at each data point. Calibrated microweights have been attached as external loads at the front end of the beam. The corresponding vertical displacements of the front end have been determined optically by a video microscope. Fig. 4 shows typical displacement-temperature characteristics.

From these measurements, the maximum force in martensitic condition  $F_{\text{mart}}$  and shape recovery force  $F_{\text{SME}}$  of the microactuator are determined to about 200 and  $850 \mu\text{N}$ , respectively. The magnetic attraction force between the front end of the beam and the magnetic core  $F_{\text{mag}}$  is estimated to about  $300 \mu\text{N}$  in deflected condition. In the planar memory shape, this force decreases to less than  $10 \mu\text{N}$ . As the optical microscanners are first prototypes, the different forces have not yet been optimized.

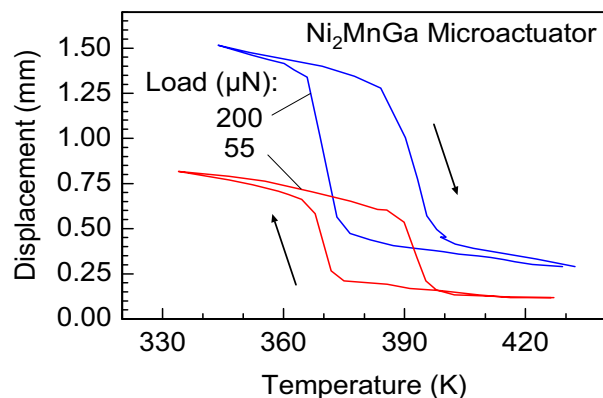


Fig. 4: Displacement-temperature characteristics of the  $\text{Ni}_2\text{MnGa}$  microactuator.

#### Optical scanning performance

Fig. 5 shows a scanned image of a laser beam directed onto the micromirror. A straight line is obtained on the screen demonstrating that no disturbing lateral movements of the double beam occur. As indicated in Fig. 5, the scanning angle  $\alpha$  is determined from the difference of minimum and maximum beam deflection.

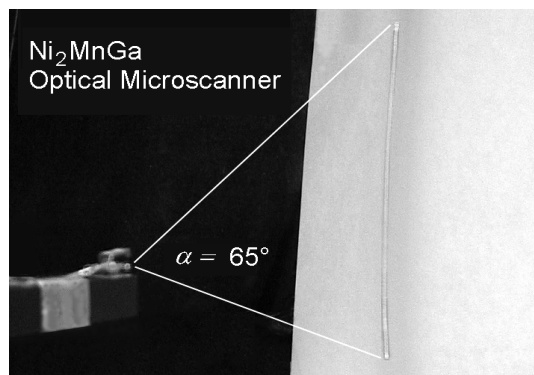


Fig. 5: Laser beam deflected by a microscanner prototype. The scanning angle is indicated by  $\alpha$ .

The dependence of scanning angle on the driving power is shown in Fig. 6. The microactuator is driven by a pulsed heating signal of 2 ms duration at a fixed frequency of 30 Hz well below the resonance frequency of 160 Hz. A pronounced hysteresis is present in the characteristic. At small driving power, the magnetic reluctance force dominates. In this case, the beam end oscillates with a relatively small amplitude close to the magnetic core. For increasing power, the oscillation amplitude increases until a critical power is reached, above which the shape recovery force dominates. In this case, oscillation of the double beam takes place close to its planar orientation.

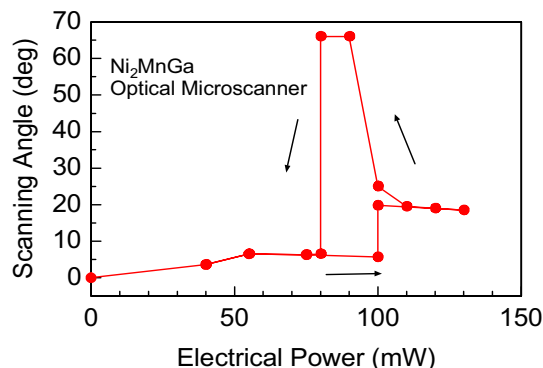


Fig. 6: Scanning angle – power characteristic of a microscanner prototype. The given power indicates the peak power of each heating pulse. The arrows indicate the course of hysteresis. The driving frequency is 30 Hz.

By decreasing the driving power again, an optimum power regime is reached, where the bi-directional actuation by magnetic and shape recovery forces generates large net-forces in both directions and thus a large stroke. In this power regime, large scanning angles up to 75 deg have been observed so far, even though the microactuator is operated off-resonance. This result outperforms specifications of previously developed microscanners, which in most cases work in resonance at a fixed frequency.

The scanning angle-frequency characteristic is shown in Fig. 7 for optimum driving power. The duration of the heating pulse signal has been kept constant at 2 ms. Below a critical frequency of about 80 Hz, the scanning angle remains almost constant. By increasing the driving frequency above the critical frequency, the scanning angle sharply decreases. This low-pass behavior is determined by the dynamics of heat transfer. From the heating time constant of the microactuator of 2 ms and the critical frequency, the corresponding cooling time constant is estimated to 10 ms. The relatively short cooling time constant is due to the high phase transformation temperatures of the used material and the size of the microactuator. Forced convective cooling during scanning motion contributes in addition to rapid cooling. For driving frequencies above the critical frequency, the heat transfer upon cooling remains incomplete, which is associated with incomplete phase transformation.

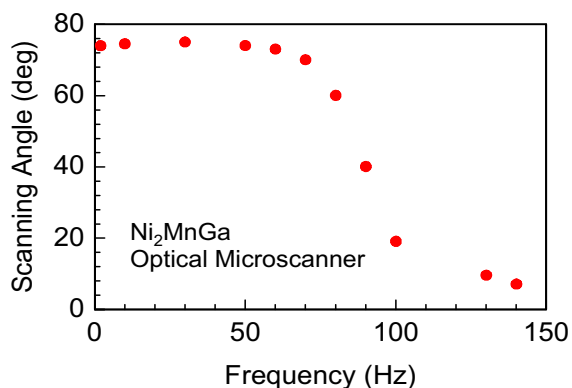


Fig. 7: Scanning angle – frequency characteristic of a microscanner prototype.

Due to operation in off-resonance mode, a considerable bandwidth of scanning frequencies is available. By reduction of microactuator size and increase of phase transformation temperatures, the critical frequency may be extended beyond 100 Hz.

### CONCLUSIONS

The multifunctional properties of ferromagnetic shape memory alloys open up new prospects for realization of smart devices and systems. For  $\text{Ni}_2\text{MnGa}$  thin films a novel actuation mechanism is proposed making use of the antagonism of intrinsic magnetic and shape recovery forces. By this mechanism, high net-forces are generated in each

actuation direction allowing a large stroke. Furthermore, compact and simple designs are possible with a large potential for miniaturization.

Based on the actuation mechanism an optical microscanner has been developed. For the used alloy composition and actuator design large scanning angles of 75 deg are obtained, which are independent of operation frequency up to a critical frequency of about 80 Hz. The critical frequency is determined by the time constants of heat-transfer upon heating and cooling the microactuator of 2 and 10 ms, respectively.

Besides optical scanning applications, the proposed actuation mechanism is expected to open up other fields of applications, where large displacements and/or forces need to be generated in small space.

### REFERENCES

- [1] K. Ullakko, J.K. Huang, C. Kantner, R.C. O'Handley and V.V. Kokorin, Large magnetic-field-induced strains in  $\text{Ni}_2\text{MnGa}$  single crystals, *Appl. Phys. Lett.* 69 (1996) 1966-1968.
- [2] R.D. James and M. Wuttig, Alternative smart materials, *Proc. of the SPIE symposium on smart structures and materials*, V.V. Varadan and J. Chandra Eds., Vol. 2715 (1996), pp. 420-426.
- [3] R.D. James and M. Wuttig, Magnetostriction of martensite, *Philosophical Magazine A*, Vol. 77, No. 5 (1998) 1273-1299.
- [4] R. Tickle and R.D. James, Magnetic and magnetomechanical properties of  $\text{Ni}_2\text{MnGa}$ . *J. of Magnetism and Magnetic Materials* 195 (1999) 627-638.
- [5] I. Aaltio and K. Ullakko, Magnetic shape memory (MSM) actuators, *Proc. of the 7<sup>th</sup> Int. Conf. on New Actuators*, Actuator 2000, Bremen, Germany, H. Borgmann Ed., (2000) pp. 527-530.
- [6] A.N. Vasil'ev, A.D. Bozhko, V.V. Khovailo, I.E. Dikshtein, V.G. Shavrov, V.D. Buchelnikov, M. Matsumoto, S. Suzuki, T. Takagi and J. Tani, Structural and magnetic phase transitions in shape memory alloys  $\text{Ni}_{2+x}\text{Mn}_{1-x}\text{Ga}$ , *Phys. Rev. B* 59, No. 2 (1999) 1113-1120.
- [7] A.N. Vasil'ev, T. Takagi, J. Tani and M. Matsumoto, Alternative applications of ferromagnetic shape memory material  $\text{Ni}_2\text{MnGa}$ , *Proc. of the Int. Symp. on Microsystems, Intelligent Materials and Robots*, Sendai, Japan (1995), pp. 423-426.
- [8] M. Suzuki, M. Ohtsuka, T. Suzuki, M. Matsumoto and H. Miki, Fabrication and characterization of sputtered  $\text{Ni}_2\text{MnGa}$  thin films, *Materials Transactions, JIM*, Vol. 40, No. 10 (1999), pp. 1174-1177.
- [9] M. Ohtsuka and K. Itagaki, Effect of heat treatment on properties of  $\text{NiMnGa}$  films prepared by a sputtering method, *Int. J. of Applied Electromagnetics and Mechanics* 12 (2000) 49-59.
- [10] C. Craciunescu, Y. Kishi, L. Saraf, R. Ramesh and M. Wuttig, Ferromagnetic  $\text{NiMnGa}$  and  $\text{CoNiGa}$  shape memory alloy films, *MRS Proc. Vol. 687* (2001).